

## Photocatalysis with Visible Light

Photocatalytic Nanodiodes for Visible-Light  
Photocatalysis\*\*

Hyun G. Kim, Pramod H. Borse, Wonyong Choi, and  
Jae S. Lee\*

Photocatalysts that respond to visible light ( $\lambda < 400$  nm) are needed to utilize the main part of the solar spectrum for production of hydrogen energy by splitting water,<sup>[1,2]</sup> purification of water and air,<sup>[3]</sup> and other applications.<sup>[4]</sup> Traditional visible-light photocatalysts are either unstable upon illumination with light (e.g., CdS, CdSe)<sup>[5]</sup> or have low activity (e.g., WO<sub>3</sub>, Fe<sub>2</sub>O<sub>3</sub>).<sup>[6]</sup> Recently, some UV-active oxides functioned as visible-light photocatalysts by substitutional doping of metals (as in MTiO<sub>2</sub> (M = Fe, V, Mn)<sup>[7]</sup> and Ni<sub>x</sub>In<sub>1-x</sub>TaO<sub>4</sub><sup>[8]</sup>), reduction of TiO<sub>2</sub> (as in TiO<sub>x</sub> ( $x < 2$ )),<sup>[9]</sup> and anion doping with N, C, and S (as in TiO<sub>2-x</sub>N<sub>x</sub>,<sup>[10]</sup> TiO<sub>2-x</sub>C<sub>x</sub>,<sup>[11]</sup> TaON,<sup>[12]</sup> and Sm<sub>2</sub>Ti<sub>2</sub>O<sub>5</sub>S<sub>2</sub><sup>[13]</sup>). However, these doped materials, in general, show a small absorption in the visible-light region, leading to low activities.<sup>[14]</sup> New and more efficient visible-light photocatalysts are needed to meet the requirements of future environmental and energy technologies driven by solar energy.

Herein we describe a novel configuration of composite solids designated as photocatalytic nanodiodes (PCD). These contain nano-islands of p-type CaFe<sub>2</sub>O<sub>4</sub> interfaced over a highly crystalline layered perovskite base lattice (n-type PbBi<sub>2</sub>Nb<sub>1.9</sub>W<sub>0.1</sub>O<sub>9</sub>), yielding nanodimensional p-n junctions.

[\*] Dr. H. G. Kim, Dr. P. H. Borse, Prof. W. Choi, Prof. J. S. Lee  
Department of Chemical Engineering and  
School of Environmental Science & Engineering  
Pohang University of Science and Technology  
San-31 Hyoja-dong, Pohang 790-784 (Korea)  
Fax: (+81) 54-279-5528  
E-mail: jlee@postech.ac.kr

[\*\*] This work was supported by the Hydrogen Energy R&D Center, the Research Center for Energy Conversion and Storage, the National R&D Center for Nano Science and Technology, the National Research Laboratory Program, and the General Motors R&D Center.



Supporting information for this article is available on the WWW under <http://www.angewandte.org> or from the author.

This nanodiode material shows greatly enhanced and stable photocatalytic activity for degradation of toxic organic pollutants (acetaldehyde, isopropyl alcohol), oxidation of water to gaseous oxygen, and photocurrent generation, all under visible light ( $\lambda > 420$  nm).

In the rational design of this composite material, we employed a combination of concepts that optimize the photocatalytic activity. It has been demonstrated in photovoltaic cells and photoelectrochemical (PEC) cells that diode structures made of n- and p-type semiconductors show greatly enhanced activities compared to devices consisting of a single semiconductor. For example, the fundamental unit of current silicon solar cells consists of p–n junctions with p-type and n-type silicon. Multijunction solar cells and PEC cells with remarkable energy conversion efficiencies have been reported.<sup>[15]</sup> Nojik constructed an n-TiO<sub>2</sub>/p-GaP diode electrode for a PEC cell that was much more active than either n-TiO<sub>2</sub> or p-GaP single-component electrodes for the decomposition of water.<sup>[16]</sup> He designated his monolithic device a p–n type photochemical diode. We attempted to create a particulate version of the p–n junction on a nanometer scale for photocatalytic applications; this junction should be stable under typical photocatalytic reaction conditions and highly active under visible light. Owing to the employment of the p–n junction concept, the nanoscale size, and the particulate form of our device material, we designated it a p–n type photocatalytic nanodiode (PCD).

The first step in fabricating the PCD was to select proper p- and n-type semiconductors that could absorb visible light. We identified PbBi<sub>2</sub>Nb<sub>2</sub>O<sub>9</sub> as a suitable n-type semiconductor. This material is an Aurivillius-phase layered perovskite, and is an efficient photocatalyst for the oxidation of water to O<sub>2</sub> and the degradation of isopropyl alcohol to CO<sub>2</sub> under visible light.<sup>[17]</sup> For PbBi<sub>2</sub>Nb<sub>2</sub>O<sub>9</sub> to show n-type semiconductivity, it was doped with tungsten(vi) to provide n-PbBi<sub>2</sub>Nb<sub>1.9</sub>W<sub>0.1</sub>O<sub>9</sub>. In addition to the valency, the similarity in size between W<sup>VI</sup> (0.74 nm) and Nb<sup>V</sup> (0.78 nm) was a further consideration in our choice. For the p-type semiconductor we chose CaFe<sub>2</sub>O<sub>4</sub>, a metal oxide with a bulk band gap of 1.9 eV.<sup>[18]</sup> The material by itself shows very low photocatalytic activity under visible light. Yet, we selected it because of its p-type semiconductivity and expected stability in water under illumination.

The next challenge was to combine these two semiconductor particles to form a p–n junction. For the efficient use of such a diode structure, the interfacing area should be maximized. However, in preliminary experiments, we learned that PbBi<sub>2</sub>Nb<sub>1.9</sub>W<sub>0.1</sub>O<sub>9</sub> must be in a highly crystalline state to obtain high activity; this requires a high-temperature synthesis that inevitably produces large particles of 0.1–1  $\mu$ m in diameter. We therefore devised the configuration of the diode particles as follows: 1) Nanocrystals of p-type CaFe<sub>2</sub>O<sub>4</sub> and 2) a perovskite lattice of n-type PbBi<sub>2</sub>Nb<sub>1.9</sub>W<sub>0.1</sub>O<sub>9</sub> as a submicron-sized base material. The CaFe<sub>2</sub>O<sub>4</sub> nanoparticles and PbBi<sub>2</sub>Nb<sub>1.9</sub>W<sub>0.1</sub>O<sub>9</sub> submicron particles were synthesized individually by sol–gel methods and a solid-state reaction, respectively. The individual components were then combined by placing them in a hydrothermal reactor (150 °C for 7 d) to form CaFe<sub>2</sub>O<sub>4</sub> nano-islands over larger particles of PbBi<sub>2</sub>Nb<sub>1.9</sub>W<sub>0.1</sub>O<sub>9</sub>.

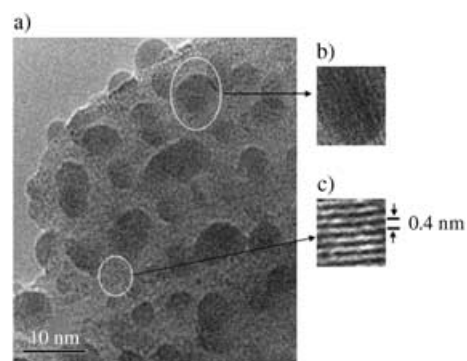


**Figure 1.** a) HRTEM image of the p–n type photocatalytic nanodiode (PCD). The magnified views show the nanocrystalline p-type CaFe<sub>2</sub>O<sub>4</sub> (b) interfaced on layers of the n-type PbBi<sub>2</sub>Nb<sub>1.9</sub>W<sub>0.1</sub>O<sub>9</sub> base (c).

Figure 1a shows a HRTEM image of a typical PCD particle. It clearly exhibits the existence of nano-islands dispersed over a single particle of perovskite base material. The micrograph shows many nanocrystalline islands of 5–10 nm, and the magnified view of a nano-island reveals the nanocrystallinity of CaFe<sub>2</sub>O<sub>4</sub> (Figure 1b). The magnified view of the fringes also demonstrates the existence of a highly crystalline, layered base material corresponding to PbBi<sub>2</sub>Nb<sub>1.9</sub>W<sub>0.1</sub>O<sub>9</sub> (layer thickness 0.4 nm, Figure 1c). The phase identification was also confirmed by elemental analysis with in situ energy-dispersive X-ray microanalysis carried out during the microscopic study.

Based on these experimental observations we propose a model for the PCD as illustrated in Figure 2a. Each island forms a nanoscale p–n junction at the interface, which plays a crucial role in the photocatalytic process. The working principle of PND is shown as an energy band model for one p–n junction (Figure 2b). At thermal equilibrium, the Fermi levels of two semiconductors align. When the device is immersed in an electrolyte, the band edges of the conduction and valence bands bend as indicated. The operation of the PCD is initiated by the absorption of the band-gap photons in both the n- and p-type semiconductors. Photogenerated holes and electrons separate under the influence of the electric field, corresponding to the energy diagram in Figure 2b. Thus,

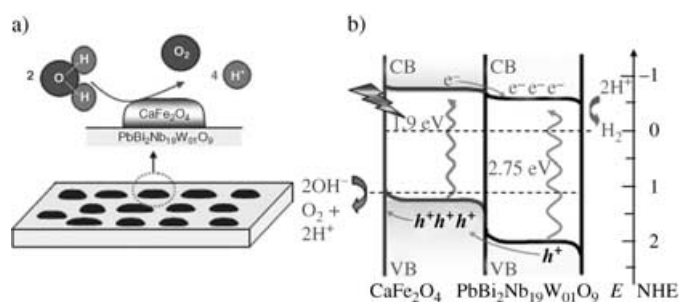


**Figure 2.** a) Schematic drawing of a PCD. b) Schematic drawing of the energy band model of a PCD showing the formation of the p–n junction and the process of water oxidation. The band positions were derived from flat band potential measurements as described in the Supporting Information. CB = conduction band, VB = valence band, NHE = normal hydrogen electrode.

holes move to the p-CaFe<sub>2</sub>O<sub>4</sub> side, and electrons to the n-PbBi<sub>2</sub>Nb<sub>1.9</sub>W<sub>0.1</sub>O<sub>9</sub> side. The net effect of the p–n diode formation is the efficient separation of electron–hole pairs to minimize the energy-wasteful electron–hole recombination. This effect leads to the higher photocatalytic activity.

The optical properties of these compounds were probed by UV/Vis diffuse reflectance spectroscopy (Figure 3 a). Then a comparison was made with the base material, PbBi<sub>2</sub>Nb<sub>2</sub>O<sub>9</sub>, and nitrogen-doped TiO<sub>2</sub>, that is, TiO<sub>2-x</sub>N<sub>x</sub>. The latter material is considered to be the standard example of a visible-light photocatalyst; the band structure of TiO<sub>2</sub> is modified by nitrogen doping to induce absorption of visible light.<sup>[10]</sup> From these spectra, we estimated the band gap energies of these materials (Table 1). The PCD powders showed a steep onset of absorption around  $\lambda=530$  nm, corresponding to green light; the band corresponding to this onset covers a major part of the visible region, compared to the other two standards considered here. The TiO<sub>2-x</sub>N<sub>x</sub> sample showed two absorption edges typical of doped materials, the main edge due to the oxide at 390 nm and a shoulder due to the nitride at 451 nm. PbBi<sub>2</sub>Nb<sub>2</sub>O<sub>9</sub> and the PCD showed single sharp edges. Thus, the PCD would absorb more visible-light photons than TiO<sub>2-x</sub>N<sub>x</sub>, although their absorption edges were almost the same around 450 nm. Both PbBi<sub>2</sub>Nb<sub>2</sub>O<sub>9</sub> and TiO<sub>2-x</sub>N<sub>x</sub> are yellow, and the PCD is orange, indicating that all these materials absorb visible light.

We then examined the photocatalytic properties of these materials. To investigate the generation of a photocurrent, aqueous suspensions of the materials containing acetate (donor) and Fe<sup>3+</sup> (acceptor) were illuminated with visible light ( $\lambda > 420$  nm).<sup>[19]</sup> Figure 3 b indicates that the PCD generates a photocurrent approximately three and five times faster than PbBi<sub>2</sub>Nb<sub>2</sub>O<sub>9</sub> and TiO<sub>2-x</sub>N<sub>x</sub>, respectively. The higher activities of PCD and PbBi<sub>2</sub>Nb<sub>2</sub>O<sub>9</sub> for photocurrent generation result from the beneficial effect of forming photocatalytic p–n nanodiodes. Unmodified TiO<sub>2</sub>, with a wide band gap, as well as all catalysts in the dark did not generate a photocurrent, as expected. The generation of photoelectrons is the critical initial step of photocatalytic reactions upon absorption of light, and the rate should directly correlate with the photocatalytic activity of the material.

The materials were then tested for the photooxidation of acetaldehyde, a hazardous air pollutant as well as a common model compound to test the photodegradation capability of photocatalysts. Figure 3 c shows the time curves of CO<sub>2</sub> evolution from the reaction  $\text{CH}_3\text{CHO} + 5/2\text{O}_2 \rightarrow 2\text{CO}_2 + 2\text{H}_2\text{O}$ . The concentration of CO<sub>2</sub> increased steadily with irradiation time at a decomposition rate of about 0.02  $\mu\text{mol h}^{-1}$  under irradiation with light. The CO<sub>2</sub> production stopped when the light was turned off and resumed at the same rate when the light was turned on again. No intermediate reaction products were detected. The superiority of the PCD over PbBi<sub>2</sub>Nb<sub>2</sub>O<sub>9</sub> and TiO<sub>2-x</sub>N<sub>x</sub>, as expected from the photocurrent generation behavior, was confirmed. Similar results were obtained for the photodecomposition of isopropyl alcohol, another common organic pollutant of air (not shown).

As the final test reaction, we studied the photodecomposition of water in the presence of sacrificial agents. These

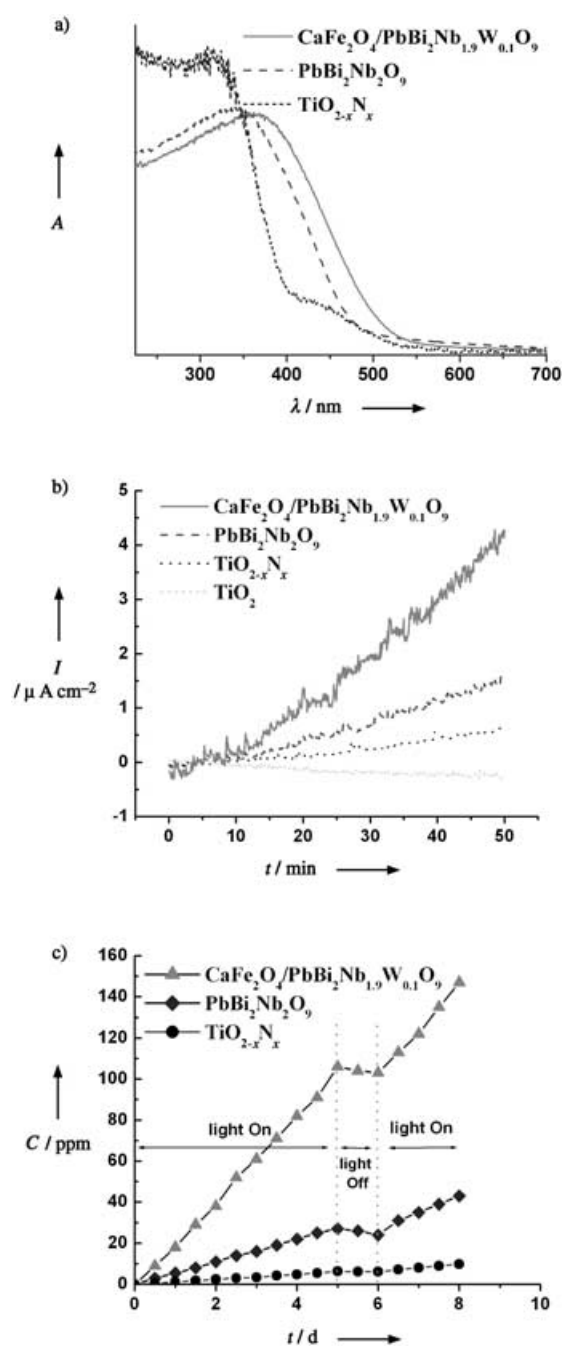


**Figure 3.** a) UV/Vis absorbance  $A$  of the various catalysts tested. b) Photocurrent  $I$  generated with time under visible light over various materials suspended with acetate and Fe<sup>3+</sup>. c) Concentration  $c$  of evolved CO<sub>2</sub> as a function of time during photooxidation of acetaldehyde with various photocatalysts (0.3 g). The acetaldehyde (200 ppm) was mixed with air in a 500-mL Pyrex reaction cell.

experiments give individual hydrogen- and oxygen-producing activities from each half-reaction of water splitting. In these reactions, two reference catalysts were loaded with 0.1 wt % Pt as a co-catalyst to collect photoelectrons away from holes by forming a Schottky-type junction structure.<sup>[16]</sup> The rates of oxygen evolution from water in the presence of AgNO<sub>3</sub> as the electron scavenger ( $2\text{H}_2\text{O} + 4\text{Ag}^+ \rightarrow \text{O}_2 + 4\text{H}^+$ ) are listed in Table 1. Again, the PCD demonstrated the best performance

**Table 1:** Photocatalytic activities for oxygen evolution from an aqueous AgNO<sub>3</sub> solution as tested for the various catalysts.<sup>[a]</sup>

Catalyst	Band gap energy		Oxygen evolution	
	E <sub>g</sub> [eV]	λ <sub>ab</sub> [nm] <sup>[b]</sup>	[μmol] <sup>[c]</sup>	QY [%] <sup>[d]</sup>
CaFe <sub>2</sub> O <sub>4</sub> /PbBi <sub>2</sub> Nb <sub>1.9</sub> W <sub>0.1</sub> O <sub>9</sub>	2.75	450	675	38
PbBi <sub>2</sub> Nb <sub>2</sub> O <sub>9</sub>	2.88	431	520	29
TiO <sub>2-x</sub> N <sub>x</sub>	2.73 <sup>[e]</sup>	451	221	14

[a] Catalyst 0.3 g; light source 450-W Xe-arc lamp (Oriel) with UV cut-off filter (λ ≥ 420 nm). The reaction was performed in an aqueous AgNO<sub>3</sub> solution (0.05 mol L<sup>-1</sup>, 200 mL). [b] The wavelength at the absorption edge was determined as the intercept on the wavelength axis for a tangent drawn on absorption spectra. [c] Per gram of catalyst and hour. [d] QY = quantum yield (see the Experimental Section). [e] The minimum energy of photoabsorption was estimated from the intercept of the shoulder peak onset.

even without a co-catalyst. The quantum yield of O<sub>2</sub> evolution over the PCD was estimated to be about 38%. To the best of our knowledge, this is the highest value ever reported for the reaction over semiconductor photocatalysts under visible light. The hydrogen evolution with methanol as a hole scavenger was also studied (H<sub>2</sub>O + CH<sub>3</sub>OH → 3 H<sub>2</sub> + CO<sub>2</sub>). The relative activity trend among the three photocatalysts was the same, but the rates were lower than those for oxygen evolution by factors of at least 10, and thus are not reported herein.

It has been demonstrated that PCD is a highly active novel photocatalyst. Application of the p–n diode concept commonly employed in the synthesis of monolithic energy conversion devices and the employment of techniques for nanomaterial synthesis have allowed the production of a nanocomposite between the high-order oxides with a unique configuration. It appears that the p–n diode formation results in the efficient separation of electron–hole pairs to minimize the energy-wasteful electron–hole recombination, which leads to the high photocatalytic activity. The materials involved are all stable oxides, which means less stability problems under irradiation with light. Indeed, the crystal structure did not change during the reaction, and the post-reaction analysis showed no indication of dissolved catalyst components, even after more than 100 h of water decomposition.

The PCD catalyst appears to be particularly active for photooxidation reactions. The activity could be directly exploited for the degradation of toxic organic pollutants, as demonstrated for acetaldehyde and isopropyl alcohol. Cheap and abundant sunlight or weak indoor lighting could be employed as the light source. The high activity for the oxidation of water and the generation of a photocurrent could be of advantage for producing a photoelectrochemical cell that converts optical energy into chemical energy by decomposing water.<sup>[2]</sup> The overall performance of such a device is determined by the ability of the semiconductor anode<sup>[2]</sup> to oxidize water, and our PCD photocatalyst with the remarkable oxygen-producing capability could be used for this purpose. Furthermore, since the concept of PCD fabrication could be applied for other visible-light absorbing semiconductors, further improvement in performance may be possible by a materials screening of a wider scope.

## Experimental Section

To synthesize the PCD, PbBi<sub>2</sub>Nb<sub>1.9</sub>W<sub>0.1</sub>O<sub>9</sub> was first prepared by the conventional solid-state method. A stoichiometric mixture of PbO (Aldrich 99.999%), Bi<sub>2</sub>O<sub>3</sub> (Aldrich 99.99%), Nb<sub>2</sub>O<sub>5</sub> (Aldrich 99.999%), and WO<sub>3</sub> (Aldrich 99.999%) was ground in a mortar. The pelletized powders were calcined at 1123 K for 24 h in static air and sintered at 1323 K for 24 h. Next, the sol–gel route was adopted to synthesize the CaFe<sub>2</sub>O<sub>4</sub> nanoparticles: A stoichiometric ratio of Ca(NO<sub>3</sub>)<sub>2</sub>·4H<sub>2</sub>O (Aldrich 99.999%) and Fe(NO<sub>3</sub>)<sub>3</sub>·9H<sub>2</sub>O (Aldrich 99.999%) was mixed in 30% aqueous NH<sub>3</sub> solution, and the mixture was stirred at room temperature for 24 h. The PCD composite of CaFe<sub>2</sub>O<sub>4</sub>/PbBi<sub>2</sub>Nb<sub>2-x</sub>W<sub>x</sub>O<sub>9</sub> was made by hydrothermal treatment of preformed PbBi<sub>2</sub>Nb<sub>1.9</sub>W<sub>0.1</sub>O<sub>9</sub> and CaFe<sub>2</sub>O<sub>4</sub> sol at 150°C for 7 d to obtain 2 wt% CaFe<sub>2</sub>O<sub>4</sub> loading on PbBi<sub>2</sub>Nb<sub>2-x</sub>W<sub>x</sub>O<sub>9</sub>. The CaFe<sub>2</sub>O<sub>4</sub>/PbBi<sub>2</sub>Nb<sub>1.9</sub>W<sub>0.1</sub>O<sub>9</sub> thus obtained was characterized by high-resolution transmission electron microscopy (HRTEM, Phillips Model CM 200) and UV/Vis diffuse reflectance spectroscopy (Shimadzu, UV 2401).

Prior to the water-splitting reactions, all the catalysts (except the PCD) were loaded with 0.1 wt% Pt by impregnation with PtCl<sub>2</sub>. The photocatalytic reactions in aqueous solution were carried out at room temperature in a closed system using a 450-W Xe-arc lamp (Oriel) with UV cut-off filter (λ ≥ 420 nm) placed in an inner irradiation-type 200-mL Pyrex reaction cell. The H<sub>2</sub> evolution was examined in an aqueous solution (distilled H<sub>2</sub>O (170 mL) + CH<sub>3</sub>OH (30 mL)), and the O<sub>2</sub> evolution in an aqueous AgNO<sub>3</sub> solution (0.05 mol L<sup>-1</sup>, 200 mL), both containing 0.3 g of the catalyst. The quantum yield (QY) was calculated as twice the number of generated H<sub>2</sub> molecules or four times the number of generated O<sub>2</sub> molecules divided by the number of photons absorbed by the photocatalyst. The number of absorbed photons was determined with a light flux meter (1815-C, Newport) with the light sensor attached to the photocatalytic reactor.

About 200 ppm of gaseous CH<sub>3</sub>CHO or isopropyl alcohol was injected into a 500-mL Pyrex reaction cell filled with air and containing 0.3 g of a catalyst. The concentration of the reaction products (H<sub>2</sub>, O<sub>2</sub>, CO<sub>2</sub>) was determined by a gas chromatograph equipped with a thermal conductivity detector and a molecular sieve 5-Å column. For photocurrent measurements, 25 mg of photocatalyst was suspended in distilled H<sub>2</sub>O (75 mL) containing acetate (0.1M) and Fe<sup>3+</sup> (0.1 mM) as an electron donor and acceptor, respectively, and the pH value of the suspension was adjusted to 1.4 with HClO<sub>4</sub>. A Pt plate (1 × 1 cm<sup>2</sup>, 0.125 mm thick, both sides exposed to solution), a saturated calomel electrode (SCE), and a Pt gauze were immersed in the reactor as working (collector), reference, and counter electrodes, respectively. With continuous N<sub>2</sub> purging of the suspension, photocurrents were measured by applying a potential (+0.6 V vs. SCE) to the Pt electrode using a potentiostat (EG&G).

Received: January 7, 2005

Revised: April 13, 2005

Published online: June 27, 2005

**Keywords:** green chemistry · nanotechnology · photocatalysis · photooxidation · semiconductors

- [1] A. Fujishima, K. Honda, *Nature* **1972**, 238, 37.
- [2] M. Gratzel, *Nature* **2001**, 414, 338.
- [3] M. R. Hoffman, S. T. Martin, W. Choi, D. W. Bahnemann, *Chem. Rev.* **1995**, 95, 69.
- [4] R. Wang, K. Hashimoto, A. Fujishima, M. Chikuni, E. Kojima, M. Shimohigoshi, T. Watanabe, *Nature* **1997**, 388, 431.
- [5] G. C. De, A. M. Roy, S. S. Bhattacharya, *Int. J. Hydrogen Energy* **1996**, 21, 19.
- [6] D. W. Hwang, J. Kim, T. J. Park, J. S. Lee, *Catal. Lett.* **2002**, 80, 53.
- [7] H. Yamashita, M. Harada, *J. Photochem. Photobiol. A* **2002**, 148, 257.

- [8] Z. Zou, J. Ye, K. Sayama, H. Arakawa, *Nature* **2001**, *414*, 625.  
 [9] R. G. Breckenridge, W. R. Hosler, *Phys. Rev.* **1953**, *91*, 79.  
 [10] R. Asahi, T. Morikawa, T. Ohwaki, K. Aoki, Y. Taga, *Science* **2001**, *293*, 269; S. Sakthivel, H. Kisch, *ChemPhysChem* **2003**, *4*, 487.  
 [11] S. U. M. Khan, M. Al-Shahry, W. B. Ingler, Jr., *Science* **2002**, *297*, 2243; S. Sakthivel, H. Kisch, *Angew. Chem.* **2003**, *115*, 5057; *Angew. Chem. Int. Ed.* **2003**, *42*, 4908.  
 [12] G. Hitoki, T. Takata, J. N. Kondo, M. Hara, H. Kobayashi, K. Domen, *Chem. Commun.* **2002**, 1698.  
 [13] A. Ishikawa, T. Takata, J. N. Kondo, M. Hara, H. Kobayashi, K. Domen, *J. Am. Chem. Soc.* **2002**, *124*, 13547.  
 [14] D. W. Hwang, H. G. Kim, J. S. Lee, J. Kim, W. Li, S. H. Oh, *J. Phys. Chem. B* **2005**, *109*, 2093.  
 [15] O. Khaselev, J. Turner, *Science* **1998**, *280*, 425.  
 [16] A. J. Nojik, *Appl. Phys. Lett.* **1976**, *29*, 150; A. J. Nojik, *Appl. Phys. Lett.* **1977**, *30*, 567.  
 [17] H. G. Kim, D. W. Hwang, J. S. Lee, *J. Am. Chem. Soc.* **2004**, *126*, 8912.  
 [18] Y. Matsumoto, *J. Solid State Chem.* **1996**, *126*, 227.  
 [19] H. Park, W. Choi, *J. Phys. Chem. B* **2003**, *107*, 3885.